

Vinylogous Dehydration by a Polyketide Dehydratase Domain in Curacin Biosynthesis

William D. Fiers,[†] Greg J. Dodge,[‡] David H. Sherman,[§] Janet L. Smith,[‡] and Courtney C. Aldrich^{*,†,§}

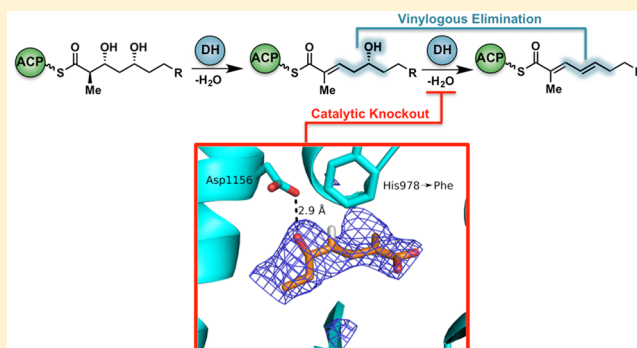
[†]Department of Medicinal Chemistry, College of Pharmacy, University of Minnesota, Minneapolis, Minnesota 55455, United States

[‡]Department of Biological Chemistry and Life Sciences Institute, University of Michigan, Ann Arbor, Michigan 48109, United States

[§]Department of Medicinal Chemistry and Life Sciences Institute, University of Michigan, Ann Arbor, Michigan 48109, United States

S Supporting Information

ABSTRACT: Polyketide synthase (PKS) enzymes continue to hold great promise as synthetic biology platforms for the production of novel therapeutic agents, biofuels, and commodity chemicals. Dehydratase (DH) catalytic domains play an important role during polyketide biosynthesis through the dehydration of the nascent polyketide intermediate to provide olefins. Our understanding of the detailed mechanistic and structural underpinning of DH domains that control substrate specificity and selectivity remains limited, thus hindering our efforts to rationally re-engineer PKSs. The curacin pathway houses a rare plurality of possible double bond permutations containing conjugated olefins as well as both *cis*- and *trans*-olefins, providing an unrivaled model system for polyketide dehydration. All four DH domains implicated in curacin biosynthesis were characterized *in vitro* using synthetic substrates, and activity was measured by LC-MS/MS analysis. These studies resulted in complete kinetic characterization of the *all-trans*-trienoate-forming CurK-DH, whose k_{cat} of 72 s^{-1} is more than 3 orders of magnitude greater than that of any previously reported PKS DH domain. A novel stereospecific mechanism for diene formation involving a vinylogous enolate intermediate is proposed for the CurJ and CurH DHs on the basis of incubation studies with truncated substrates. A synthetic substrate was co-crystallized with a catalytically inactive Phe substitution in the His-Asp catalytic dyad of CurJ-DH to elucidate substrate–enzyme interactions. The resulting complex suggested the structural basis for dienoate formation and provided the first glimpse into the enzyme–substrate interactions essential for the formation of olefins in polyketide natural products. This examination of both canonical and non-canonical dehydration mechanisms reveals hidden catalytic activity inherent in some DH domains that may be leveraged for future applications in synthetic biology.



INTRODUCTION

Polyketide secondary metabolites are an exquisite example of Nature's rich diversity, in terms of both molecular complexity and functionality. Small molecules from this natural product family cover a wide range of marketed medicinal agents, providing utility as hypolipodemic (lovastatin), antimicrobial (erythromycin), antineoplastic (ixabepilone), antifungal (amphotericin B), and immunosuppressive (FK-506) therapeutics. The variety in polyketide biological activity is largely attributed to their structural diversity arising from their assembly-line construction by polyketide synthases (PKSs). Type I PKSs consist of modular cassettes of megaenzymes with catalytic domains for extending, editing, and transferring polyketide chains. The minimal components necessary for elongation of a polyketide intermediate include an acyl carrier protein (ACP), acyltransferase (AT), and ketosynthase (KS) domains. Each module may additionally house processing domains that alter the substituents and oxidation states at the α - and β -centers. These include C-methyltransferase (CMT), ketoreductase (KR), O-methyltransferase (OMT), dehydratase

(DH), and enoyl reductase (ER) domains affording α -alkylated, β -hydroxy, β -methoxy, α,β -unsaturated, or α,β -saturated products. Many of these transformations result in stereoselective formation of an optically enriched product. Subsequent elongation and processing steps by the downstream modules lead to the mature polyketide chain. Chain termination by a thioesterase (TE) domain results in lactonization or hydrolysis to a macrolactone or carboxylic acid, respectively. The released polyketide is often subjected to tailoring events catalyzed by post-PKS tailoring enzymes that further diversify the natural product scaffold.

Curacin A, a mixed polyketide–non-ribosomal peptide natural product isolated from the cyanobacteria *Moorea producens* (formerly *Lyngbya majuscula*), is a potent anti-proliferative agent that arrests mitosis through the inhibition of tubulin polymerization.¹ Curacin A is biosynthesized via a mixed non-ribosomal peptide synthetase–polyketide synthase

Received: September 17, 2016

Published: November 16, 2016

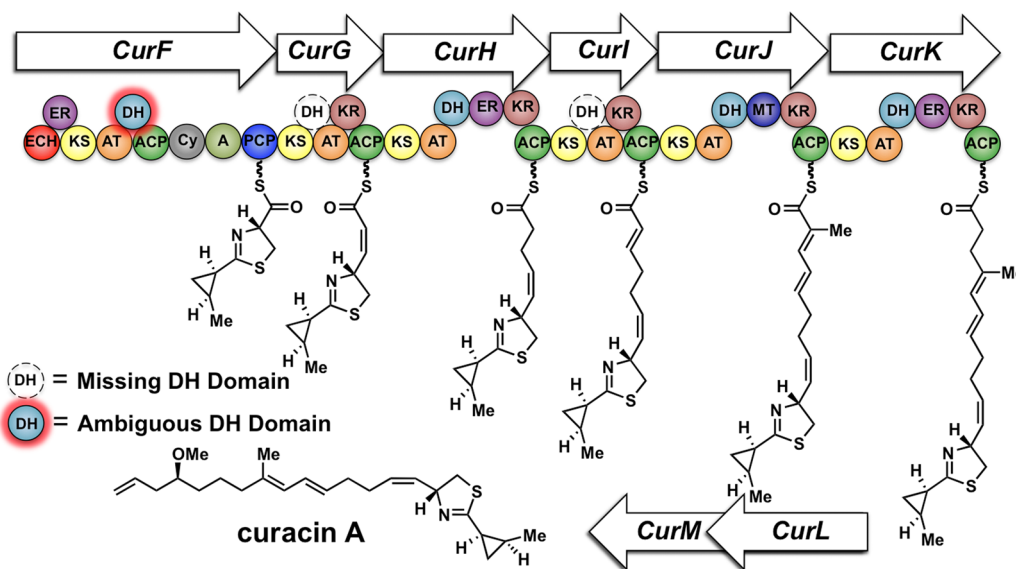


Figure 1. Curacin A mixed NRPS-PKS biosynthetic pathway. The extraneous CurF dehydratase (DH) with no predicted function is highlighted in red. The absent DHs in CurG and CurI are shown with dashed lines in black and white.

(NRPS-PKS) pathway incorporating three malonyl-coenzyme-A (CoA) units in a cyclopropyl moiety, one L-cysteine in a thiazolidine-forming cyclization reaction, and seven units of malonyl-CoA through KS-catalyzed Claisen condensations. Both C-methyl and O-methyl substituents arise from 2 equiv of S-adenosylmethionine (SAM) during PKS processing steps. The curacin (Cur) biosynthetic pathway has provided a wealth of information about non-canonical enzymatic processes in polyketide biosynthesis, including a GCN5 (yeast histone)-related N-acetyltransferase (GNAT)-like strategy for polyketide chain initiation, cyclopropane synthesis through β -branching and cryptic halogenation, as well as polyketide release via off-loading of a terminal alkene.^{2–4} Moreover, the Cur pathway has yielded tremendous structural insight into this unprecedented PKS chemistry, and three-dimensional structures of 14 proteins in the Cur pathway have been published.^{5–13}

We selected the curacin biosynthesis as a platform for studying DH activity in PKSs. The pathway uniquely produces nearly every possible type of olefin substitution pattern (mono-, di-, and trisubstituted) as well as both *cis* and *trans* geometric isomers (Figure 1). Additionally, curacins B and C constitute geometric isomers of curacin A and suggest a degree of pathway flexibility in regard to olefin formation (Figure 2).¹⁴ Bioinformatic analysis of the curacin gene cluster shows that PKS modules CurG and CurI are missing DH domains, while CurF contains an extraneous DH domain.^{10,15} Neighboring curacin modules could potentially accommodate for the missing DHs. This process, termed “domain stuttering”, involves direct transfer of an ACP-bound intermediate to the ACP of the next domain.¹⁶ This product could be β -processed (dehydrated by a DH, in this case) and then transferred back to the KS domain of the same module for a typical round of extension and β -processing. We hypothesized that these non-canonical dehydration events may occur through a simpler and more efficient process by an alternative mechanism. The Smith group previously disclosed the structural characterization of all four excised DH domains from CurF, CurH, CurJ, and CurK, providing a solid structural foundation and a unique opportunity to capture a bound substrate.¹⁰ The conserved, catalytic His-Asp dyad residues necessary for *syn*-dehydration

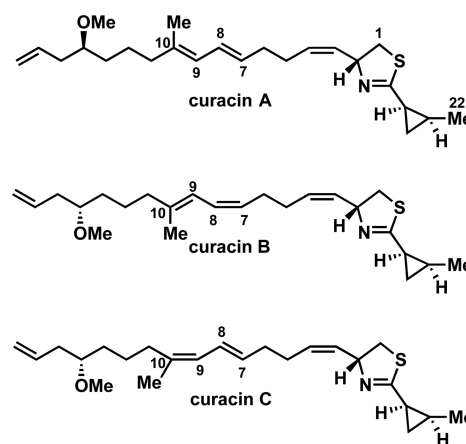


Figure 2. Natural geometric isomers of curacin. Both the $\Delta^{7,8}$ and $\Delta^{9,10}$ *cis*-isomers of curacin A have been isolated from *Moorea producens*. The biosynthetic origin of these isomerizations remains unknown.

and the active-site channels are surprisingly quite similar, giving few clues to the identity of their native substrates.^{17,18} This set the stage for our present study using synthetic substrates to probe the substrate specificity and dehydration mechanism.

RESULTS

Substrate Design and Synthesis. We set out to synthesize potential substrates to profile the dehydratase activity of the four DH domains in the pathway (Figure 3). The distal thiazolidine and cyclopropyl moieties were eliminated to reduce molecular complexity and enhance solubility of the substrates. Synthesis of the truncated CurK-DH tetraketide **1** began with a Horner–Wadsworth–Emmons reaction between *trans*-2-pentenaldehyde (**9**) and triethyl 2-phosphonopropionate (**10**) to afford the *trans,trans*-dienoate **11** in quantitative yield (Scheme 1A). The dienolate was reduced with diisobutylaluminum hydride (DIBAL-H) and oxidized to aldehyde **13** employing MnO₂. Asymmetric aldol reaction of **13** with Nagao’s D-valine-derived thiazolidinethione **14** provided

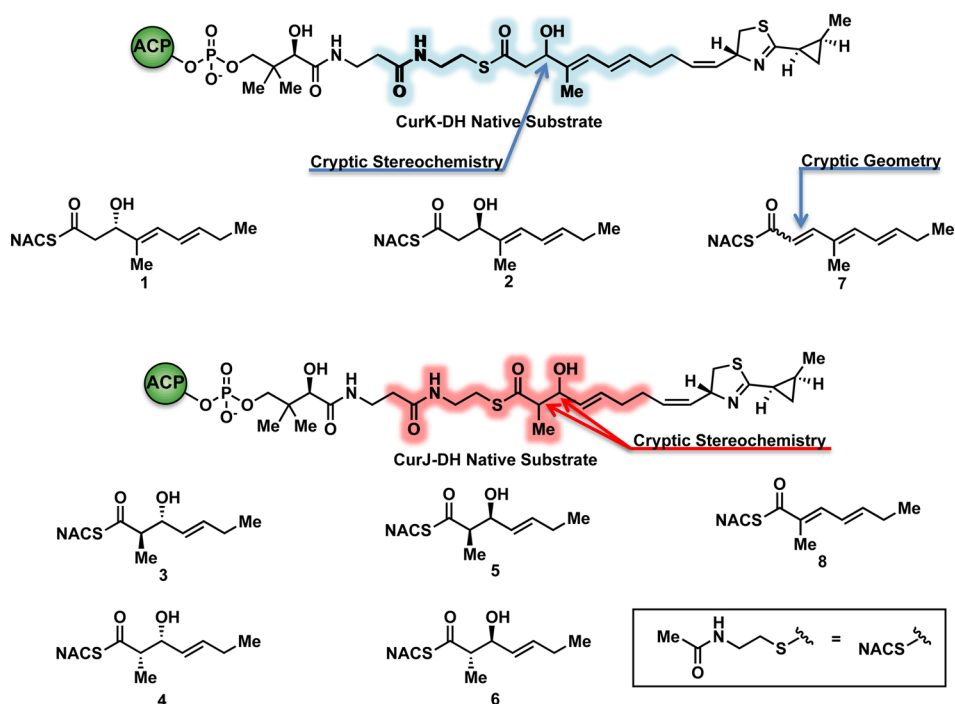
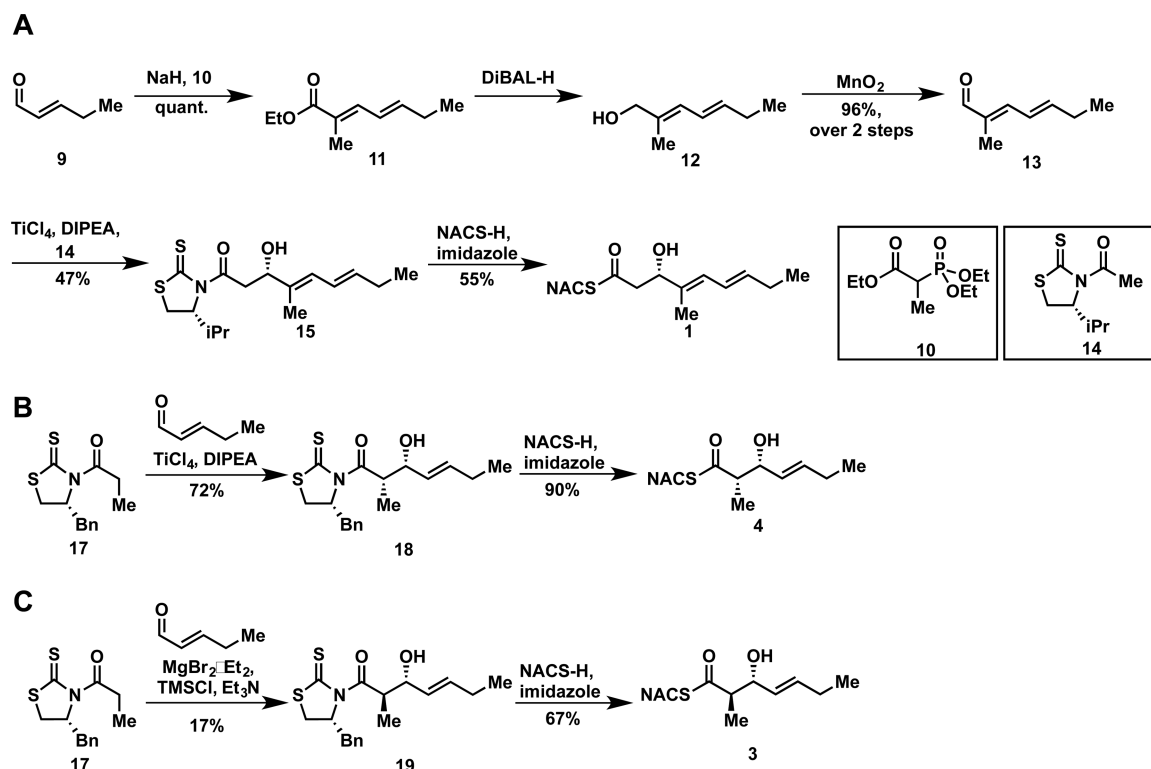


Figure 3. CurJ and CurK truncated substrates and products.

Scheme 1. Synthesis of CurK-DH Substrate 1 and the CurJ Substrates 3 and 4^a



^aAbbreviations: DIBAL-H, diisobutylaluminum hydride; DIPEA, diisopropylethylamine; NAC, *N*-acetylcysteamine.

alcohol 15 as a single diastereomer.¹⁹ Facile displacement of the chiral auxiliary with *N*-acetylcysteamine (NAC) furnished 1. The enantiomeric tetraketide 2 was prepared in an analogous fashion using the *L*-valine-derived thiazolidinethione (Supporting Information). The CurK product 7 was obtained chemoenzymatically from 1 employing CurK-DH.

The truncated CurJ triketide substrates were synthesized using Crimmins's and Evans's aldol chemistry that allows access to all four possible stereoisomers from common intermediate 9 and the *D*-phenylalanine-derived thiazolidinethione 17 or its enantiomer by varying the Lewis acid and amine base (Scheme 1).^{20,21} The *syn*-aldol adduct 18 was obtained in a respectable

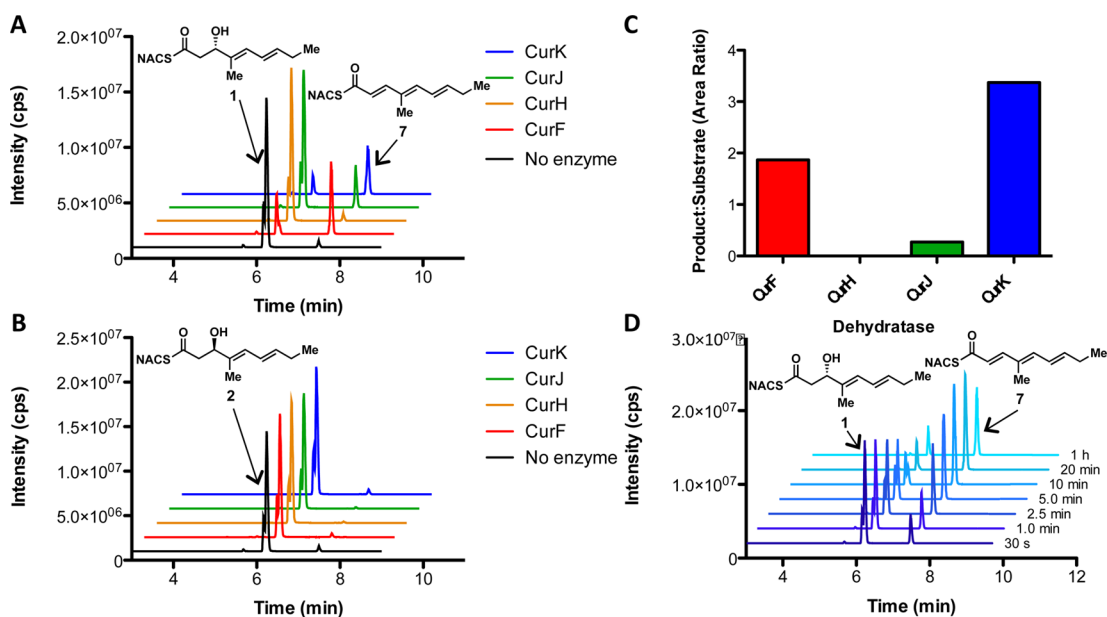


Figure 4. Incubation studies of synthetic CurK-DH substrates **1** and **2**. (A,B) Extracted chromatograms of 14 h incubations of all curacin DH domains with substrates **1** (A) and **2** (B). CurF-DH, CurJ-DH, and CurK-DH all display stereospecificity for D-alcohol (**1**) over the L-alcohol (**2**). (C) Ratio of peak areas (7:1) for each curacin dehydratase enzyme subtracting negative control (no enzyme). CurF-DH and CurK-DH efficiently produce the triene **7**, with a lesser amount produced by CurJ-DH. (D) Time course extracted chromatograms of CurK-DH ($5 \mu\text{M}$) with substrate **1** (1 mM). The enzyme reaches equilibrium by 20 min. The transition $m/z 268 \rightarrow 121$ was used to monitor both residual substrates (**1** and **2**) as well as product (**7**) formation for all extracted chromatograms due to spontaneous dehydration of the substrate under the MS ionization conditions. The recurring shoulder on compounds **1** and **2** is believed to be minor *trans,cis*-isomers arising from isomerization during assay conditions.

72% yield and converted to the required NAC thioester **4** by treatment with *N*-acetylcysteamine (Scheme 1B). The *anti*-aldol adduct **19** was isolated in 17% yield and analogously elaborated to the NAC thioester **3** (Scheme 1C). We attribute the consistently poor yield of the *anti*-aldol transformation to a limitation of the Evans's methodology when using aliphatic enals with an exchangeable γ -proton that may polymerize under the reaction conditions. The enantiomers of **3** and **4** were synthesized in an analogous way utilizing L-phenylalanine-derived thiazolidinethione auxiliary to afford **6** and **5**, respectively (Supporting Information). Additionally, the truncated CurJ product **8** was synthesized through a Horner–Wadsworth–Emmons reaction (Supporting Information).^{22,23}

Biochemical Characterization of Cur DHs with **1 and **2**.** The four recombinant dehydratase domains (CurK-DH, CurJ-DH, CurH-DH, and CurF-DH) were individually incubated overnight at 37°C with NAC esters **1** and **2** and analyzed via liquid chromatography–tandem mass spectrometry (LC-MS/MS). CurK-DH dehydrated its truncated substrate in a completely stereospecific fashion, selectively acting only on the D-alcohol **1** with no turnover for L-alcohol **2**, whereas CurH-DH was unable to process either **1** or **2** (Figure 4A,B). This matches the predicted stereospecificity of the CurK-KR containing the signature LDD motif for B-type keto-reductases.²⁴ Curiously, CurF-DH and CurJ-DH also turned over **1**, but not **2**, in a stereospecific fashion. While CurF-DH maintained comparable total conversions with that of CurK-DH (55% of CurK-DH), the CurJ-DH was drastically deficient in its ability to catalyze the same transformation (7% of CurK-DH) (Figure 4C). A single reaction product from **1** and CurK-DH was observed, which was isolated in 25% overall yield from the overnight reaction mixture. The dehydrated substrate was analyzed via ^1H and ^{13}C NMR and confirmed as the *all-trans*-

trienoate **7**. This result is consistent with the empirically based prediction that the enzymatic dehydration of D-alcohols affords *E*-olefins.^{25,26} A time course study of the dehydration of **1** (1 mM) by CurK-DH ($5 \mu\text{M}$) revealed that the enzyme rapidly dehydrates nearly all of the substrate, reaching completion within 20 min (Figure 4D). Steady-state kinetic analysis of the CurK-DH-catalyzed dehydration of **1**–**7** was quantified by LC-MS/MS under initial velocity (v_0) conditions (Experimental Section). The resulting saturation curve (v_0 versus $[\mathbf{1}]$) was fit to the Michaelis–Menten equation to provide an apparent K_M of $12.0 \pm 4.7 \text{ mM}$ and k_{cat} of $72 \pm 21 \text{ s}^{-1}$, resulting in a specificity constant (k_{cat}/K_M) of $(6.00 \pm 1.41) \times 10^3 \text{ M}^{-1} \text{ s}^{-1}$. While the K_M value is similar to those of other NAC thioester substrates with their cognate excised PKS DH domains, the k_{cat} value is nearly 3 orders of magnitude greater than that of any previously characterized PKS DH domain.^{27,28}

To probe the reaction mechanism and facilitate co-crystallization with substrates, we prepared catalytically inactive point mutants His996Phe and Asp1169Asn of the His-Asp catalytic dyad in CurK-DH based on sequence alignment and the reported CurK-DH structure.¹⁰ The His996Phe mutant was devoid of activity while the Asp1169Asn mutant retained small, but measurable activity showing 2–3% conversion of **1** to **7** after 12 h. Crystal structures of both His996Phe and Asp1169Asn CurK-DH mutants were determined at 1.4 and 1.65 Å resolution, respectively (Table 1).¹⁰ The structures of the mutant proteins were virtually identical to the wild type CurK-DH (RMSD = 0.11 Å for 509 C α atoms) with no significant conformational changes in the active site. Co-crystallization trials of substrate **1** and either mutant of wild-type CurK-DH resulted in no crystal growth under conditions that readily yielded crystals in absence of substrate. Crystal soaking experiments with **1** resulted in a rapid dissolution of the

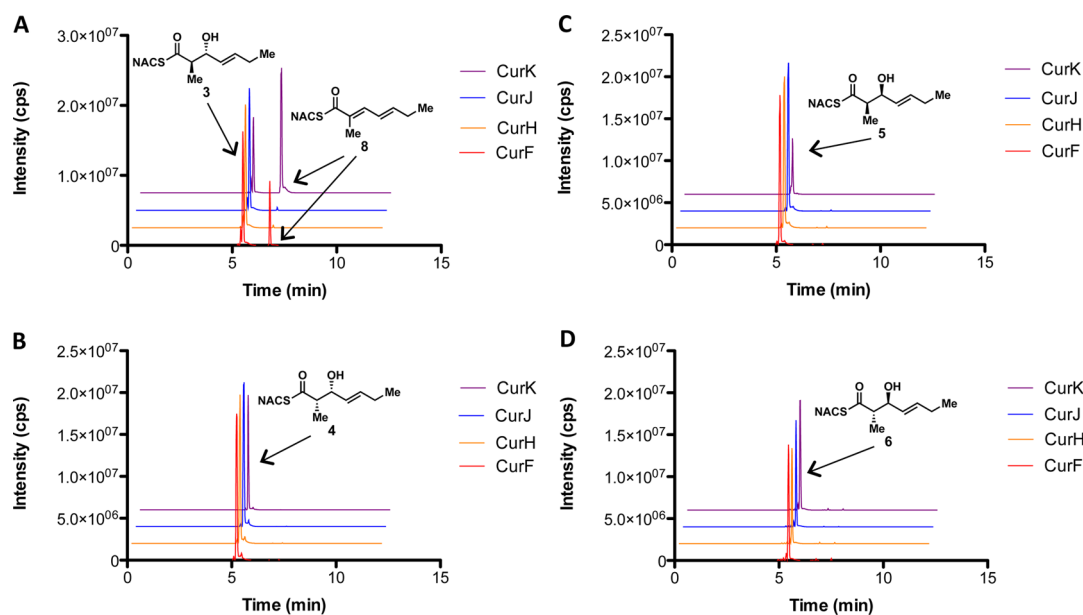


Figure 5. Overnight incubations of the putative triketide CurJ-DH substrates with all curacin PKS DHs. LC-MS/MS extracted ion chromatograms with diastereomers 3 (A), 4 (B), 5 (C), and 6 (D). In each panel, the LC-MS/MS extracted ion chromatograms are stacked with the traces for each enzyme color-coded: red for CurF, orange for CurH, blue for CurJ, and purple for CurK. The transition m/z 242 \rightarrow 95 was used to monitor both remaining substrate as well as product formation due to spontaneous dehydration under the MS ionization conditions. The *anti*-triketide 3 (panel A) is the only substrate that showed turnover by the appearance of a peak at 6.8 min corresponding to the dehydration product (this was only observed with CurK-DH and CurF-DH).

crystals, suggesting that substrate binding may induce a conformational change and destabilize the crystal form.

CurK-DH and CurF-DH Outcompete CurJ-DH in the Dehydration of Its Predicted Substrate. We next evaluated the diastereomeric triketide substrates 3–6 with all four Cur DHs (Figure 3). Interestingly, only CurK-DH and CurF-DH were able to turn over the predicted CurJ-DH substrate 3, arising from the B1-type CurJ-KR, affording the conjugated *trans,trans*-dienoate 8 (Figure 5A).²⁹ Neither of the *syn*-triketide substrates 4 and 5 nor the *anti*-triketide 6 was processed by any of the Cur DHs (Figure 5B–D). This reaffirms the substrate specificity of CurF-DH and CurK-DH for *D*-configured alcohols at the β -position. The *trans*-olefin can only be formed through a *syn*-elimination of the α -proton and β -hydroxy group in 3 and thus provides the first confirmation for this mechanism for a PKS substrate lacking an α -substituent. From a biosynthetic perspective, the inability of CurJ-DH to process any of the truncated triketide substrates was unexpected, especially in light of the high activity of CurK-DH with its predicted truncated tetraketide substrate 1. This is in stark contrast to CurJ-DH's ability to accommodate substrate 1, a *D*-alcohol lacking an α -substituent, albeit with marginal catalytic efficacy. Furthermore, these results rule out the classic “stuttered” dehydration pathway because the same substrate would be used for the second elimination. As both CurH and CurJ immediately follow modules without DH domains (i.e., CurG and CurI), we sought an alternative hypothesis for dehydration.¹⁰

CurJ-DH and CurH-DH Harbor Vinylogous Dehydration Activity. The simplest proposal is that the KR products from modules lacking DHs are carried through to the next module. After extension and reduction, the resulting β,δ -dihydroxy thioester could first be eliminated in the normal fashion (α, β) followed by a vinylogous elimination (γ, δ) yielding the diene (Figure 6). Truncated δ -hydroxy- α,β -unsaturated thioester substrates 20 and 21 were synthesized

to test this hypothesis (Supporting Information and Figure 6). No dehydration products were observed upon incubation with the *L*-alcohol substrate 20 (Figure 7A). Overnight incubation with all four DH domains revealed that only CurH-DH and CurJ-DH were able to stereospecifically process the *D*-alcohol substrate 21 to afford the *trans,trans*-dienoate product 8 (Figure 7B). Since the reaction is theoretically reversible, we next investigated the hydration reaction through incubation of *trans,trans*-dienoate 8 with each Cur DH domain. Consistent with the previous results, only CurH-DH and CurJ-DH were able to catalyze the reverse reaction, namely the regioselective and stereospecific conversion of *trans,trans*-dienoate 8 exclusively to 21 when compared to controls, albeit at a low total conversion (<1%) (Figure 7C). Both the inability of the enzyme to reach a stable equilibrium and the markedly slow reaction rate compared to the α,β -dehydration catalyzed by CurK indicate that the truncations of substrate 21 severely attenuate enzyme reactivity. The mechanism of this novel elimination was then probed through site-directed mutagenesis of the His-Asp catalytic dyad in both CurH-DH and CurJ-DH. In this case, the catalytic histidine was mutated to alanine and phenylalanine to afford CurH(H971A), CurH(H971F), CurJ(H978A), and CurJ(H978F) mutants. Similarly, the catalytic aspartate was mutated to asparagine yielding CurH(D1136N) and CurJ(D1156N). All mutants were completely devoid of activity toward 21 highlighting their critical role in this novel elimination reaction (Figure 7D).

To visualize the binding of a vinylogous substrate to a DH, 21 was co-crystallized with the catalytically inactive H978F variant of the CurJ-DH. Crystals grew more slowly in the presence of compound (30 days compared to 2 days without substrate). In the 2.4 Å structure of the DH dimer, new density appeared in the active site of one monomer, adjacent to Asp1156 and within the hydrophobic substrate tunnel (Figure 8). Strong density was present for only the acyl portion of 21,

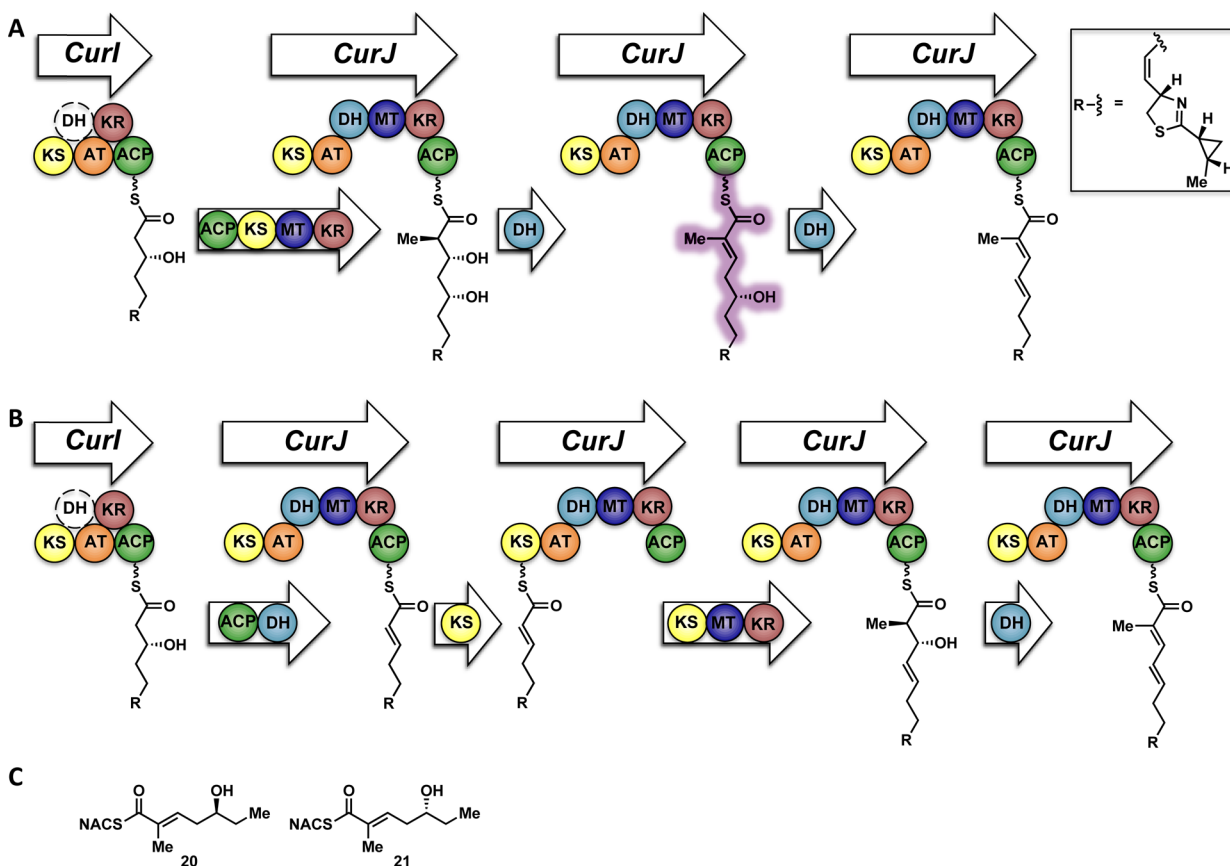


Figure 6. Proposed routes for elimination in the case of missing dehydratases. (A) Our proposed vinyllogous elimination route in module J. The polyketide intermediate from CurI is loaded onto CurJ for normal extension, methylation, and ketoreduction. The CurJ-DH eliminates the β -alcohol followed by a subsequent elimination of the δ -alcohol. (B) Classical stuttering mechanism based on predictions in other biosynthetic pathways. The polyketide intermediate from CurI is transferred directly onto the CurJ-ACP and dehydrated by the CurJ-DH. The ACP-bound intermediate is then transferred to the CurJ-KS for normal extension, methylation, and ketoreduction. A final dehydration by CurJ-DH furnishes the putative CurJ product. (C) Enantiomeric vinyllogous CurJ-DH substrates **20** and **21**. The design of the vinyllogous substrates is based on the putative native substrate shown highlighted in violet in panel A.

and we assume that the polar NAC was hydrolyzed during the long crystal growth period. The substitution of Phe for the catalytic His978 resulted in no change to the protein backbone conformation. The best fit of hydrolyzed **21** to the new density placed the δ -OH group within hydrogen bonding distance of Asp1156, in the same position as a water molecule in the free-enzyme structure.¹⁰ The acid **21** was bound such that dehydration would proceed via the classic *syn* elimination mechanism of both PKS and fatty acid synthase (FAS) DHs.

DISCUSSION

Enigmatic Dehydration in Polyketide Synthases.

Curiously, there are numerous examples in the literature of missing DH domains when diene final products or intermediates are predicted. Notable cases come from the biosynthesis of columbamides, stigmatellin, epothilones, leinamycin, thuggacin, and the myxalamides (Figure 9).^{30–34} Unexpectedly, many of these anomalies involve the formation of a *cis*-alkene during the distal dehydration. The classic interpretations of these cases invoke either a *trans*-acting DH, separate from the PKS pathway, or a stuttered dehydration process.^{30,35} Vinyllogous dehydration of δ -hydroxy- α,β -unsaturated thioester substrates as described here provides an alternative mechanism.

Crystal Structures and Substrate Specificity.

The crystallization behavior of both CurK-DH and CurJ-DH in the presence of NAC-linked substrates is suggestive of a conformational change in the protein at the entrance to the substrate tunnel. For both DHs, crystals either did not grow in the presence of substrate or grew only after thioester hydrolysis. Similarly, pre-grown DH crystals dissolved when presented with substrate. The structure of CurJ-DH H978F with the hydrolyzed **21** reveals an ideal orientation for hydrogen bonding of the catalytic Asp1156 carboxylate with the substrate hydroxyl. The site is occupied by a water molecule in structures of the DH free enzyme.¹⁰ We found that the best fit of hydrolyzed **21** to the experimental density was in a conformation that would yield a *trans,cis*-dienoate. As CurJ-DH produced the *trans,trans*-dienoate from **21** (Figure 7B), we assume that hydrolysis of the NAC thioester accounts for the predominant bound conformation.

Mechanistic Analogy to Canonical Eliminations in Dehydratase Domains.

Vinyllogous dehydration by DH domains closely parallels canonical dehydrations. Stereospecificity appears to be maintained between the two events in the module. Moreover, the empirical trend that *D*-alcohols form *E*-substituted olefins holds true in this distal elimination. The catalytic His-Asp dyad is essential for this novel, second transformation by the DH domain as the respective point

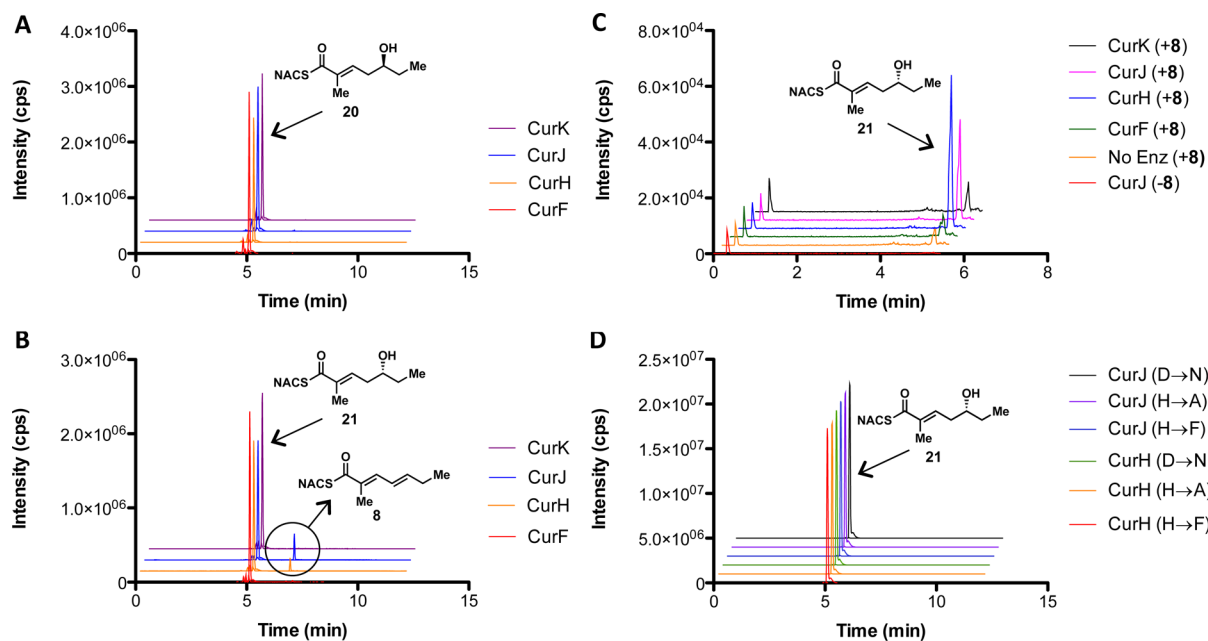


Figure 7. Vinylogous elimination of δ -hydroxy- α,β -unsaturated thioester substrates by curacin DH domains. (A,B) LC-MS/MS extracted ion chromatograms obtained after overnight incubations of substrates **20** (A) and **21** (B) with each Cur DH monitoring the transition at m/z 242 \rightarrow 95 for product dienoate **8** (peak at 6.8 min) and m/z 260 \rightarrow 141 (peak at 5.1 min) for the residual substrates. In each panel, the LC-MS/MS extracted ion chromatograms are stacked with the traces for each enzyme color-coded: red for CurF-DH, orange for CurH-DH, blue for CurJ-DH, and purple for CurK-DH. The L-alcohol substrate **20** shown in panel A is not a substrate for any of the Cur DHs, whereas the D-alcohol substrate **21** shown in panel B is converted to the corresponding dienoate **8** only by CurJ-DH and CurH-DH. (C) Hydration of dienoate **8**. Compared to negative control (without **8** or without CurJ-DH), only CurH-DH and CurJ-DH form **21** in the presence of **8**. (D) Overnight incubation of the six CurJ-DH and CurH-DH catalytic dyad point mutants, scanning for the same transitions as previous panels. All mutants are devoid of activity, as evidenced by the absence of a peak at 6.8 min.

mutants are catalytically incompetent. Given these results, we predict the reaction is a net *syn*-elimination as previously established in α,β -dehydrations in PKS and FAS systems.^{36,37} The proposed mechanism shares similarities to three reported biosynthetic enzymes: FabA, an isomerizing DH involved in coralopyronin A biosynthesis, and a recently characterized isomerase (Figure 10).^{18,38,39} The first step involves deprotonation of the γ -proton, *pro-R* in the case of FabA, by a general base (likely the catalytic His) to afford a vinylogous enolate.⁴⁰ Until this point, the reaction mechanism mirrors that of a classic isomerase. Instead of suprafacial protonation at the α -position, the subsequent elimination occurs with simultaneous protonation of the δ -hydroxyl group by the catalytic aspartic acid residue, forming the γ,δ -olefin. The dual activities would require that the substrate shift in the active site tunnel first to place the α -position by the catalytic His and the β -hydroxy by the catalytic Asp for the canonical dehydration, and then the γ -position by the catalytic His and δ -hydroxy by the catalytic Asp for the vinylogous dehydration.

In the present study, we found that CurF-DH activity unexpectedly closely mirrors that of the CurK-DH in its stereospecific processing of **1** over **2**. This seemingly nonsensical mimicry of dehydration activity is puzzling due to the fact that CurK-DH is predicted to process the longest DH substrate in the Cur pathway, and CurF-DH has no known function. By analyzing CurF polyketide cassette (ER-KS-AT-DH) against other possible pathways in the producing organism, we found that JamJ from the jamaicamide pathway has high homology (>72% identical), and the predicted action in its pathway matches that of the extra modules in CurF (i.e., a complete reductive processing sequence to form an alkane

intermediate). The majority of the modules needed for jamaicamide synthesis appear to be vestigial in CurF, and *vice versa*. For example, the ER domain is responsible for cyclopropane formation in curacin biosynthesis, whereas the vestigial JamJ ER domain has no activity with the natural jamaicamide β,γ -olefin intermediate but has robust reductive activity with α,β -olefin substrates.² Additionally, there is an NRPS module set (PCP-A-Cy) for thiazoline production appended to the end of the vestigial CurF PKS module. Genetic analysis of several PKS biosynthetic clusters has recently revealed that analogous instances of surplus DH domains present in a pathway compared to a predicted activity is a more common occurrence than missing DH domains. This often arises due to two unique evolutionary pressures: The necessity to retain a hydroxyl group in the pathway for the final natural product or the duplication and insertion of a full or partial module cassette to fulfill another pathway role. In the former case, the DH domain is often catalytically inactivated by a knockout mutation in the catalytic region. Classic examples include rifamycin (DH2 and DH5), amphotericin B (DH15, DH17, and DH18), and FK506 (DH3, DH4, and DH8).^{41–43} The latter case is often harder to interpret biosynthetically, as the partial module harbors necessary activity for the natural product biosynthesis (i.e., CurF ER), but also a superfluous and active DH domain (i.e., CurF-DH). Examples include rifamycin (DH6, DH7, and DH8), epothilone A and B (DH7 and DH8), and FK506 (DH2).^{41,43–45} Our results indicate this may be diagnosed by both sequence comparison to other modules in the organism and substrate–dehydratase interrogation, looking for high sequence identity and unexpected substrate selectivity, respectively.

Table 1. Crystallographic Information

	CurJ H978F	CurK H996F	CurK D1169N
Data			
space group	$P2_12_12_1$	$P2_12_12_1$	$P2_12_12_1$
unit cell a, b, c (Å)	47.55, 70.58, 176.02	38.11, 94.57, 152.00	38.22, 94.51, 151.70
wavelength (Å)	1.000	1.000	1.000
d_{\min} (Å)	2.4 (2.486–2.4)	1.428 (1.479–1.428)	1.648 (1.707–1.648)
observations (#)	302 198 (30 140)	1 300 944 (96 298)	860 172 (75 239)
unique reflections (#)	23 985 (2331)	100 090 (8843)	67 404 (6535)
mean I/σ_I	18.08 (2.07)	28.15 (2.74)	25.41 (2.07)
R_{merge}	0.09 (1.44)	0.04 (0.72)	0.05 (1.10)
$CC_{1/2}$	0.99 (0.77)	1.00 (0.83)	1.00 (0.70)
CC^*	1.00 (0.93)	1.00 (0.95)	1.00 (0.91)
completeness (%)	100 (100)	97 (87)	100 (99)
Wilson B (Å ²)	62.4	19.4	26.5
Refinement			
reflections (#)	23 944 (2304)	100 088 (8843)	67 401 (6535)
R_{work}	0.188 (0.349)	0.20 (0.25)	0.20 (0.28)
R_{free}	0.242 (0.376)	0.22 (0.29)	0.23 (0.31)
RMSD bonds (Å)	0.009	0.013	0.01
RMSD angles (Å)	1.06	1.32	1.21
atoms (#)			
protein	4587	4444	4436
solvent	22	168	46
ligand	11	0	0
avg B -factors (Å ²)			
protein	111	27.6	36.2
solvent	99.8	30	30.4
ligand	62.6	n/a	n/a
Ramachandran			
favoured (%)	97.3	98	97.4
allowed (%)	2.2	1.6	2.6
outliers (%)	0.5	0.4	0.0

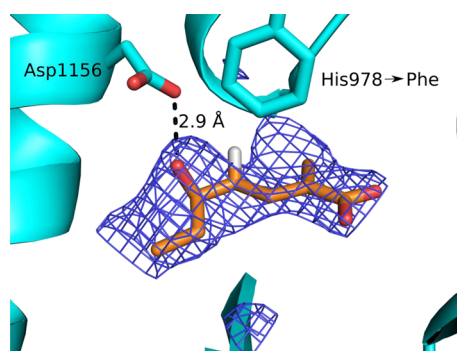


Figure 8. CurJ-DH H978F variant co-crystallized with the hydrolyzed form of compound 21. The δ -hydroxyl group of carboxylate 21 is within hydrogen bonding distance of Asp1156 (blue SA omit electron density contoured at 2.5σ). Hydrolyzed 21 (sticks with atom coloring: orange, C; red, O; white, H; only the *pro-R* H atom is shown) is within 4 Å of the Phe substitution for His978 (sticks with cyan, C).

CONCLUSION

The curacin biosynthetic pathway continues to provide unique insight into non-canonical PKS enzymology. The present study focused on the mechanism and timing of DH-catalyzed processing in assembly of the polyketide segment introduced by the five Cur PKS monomodules, CurG–CurK. Retro-biosynthetic analysis indicated that five dehydrations are required; however, DH domains are missing in both CurG

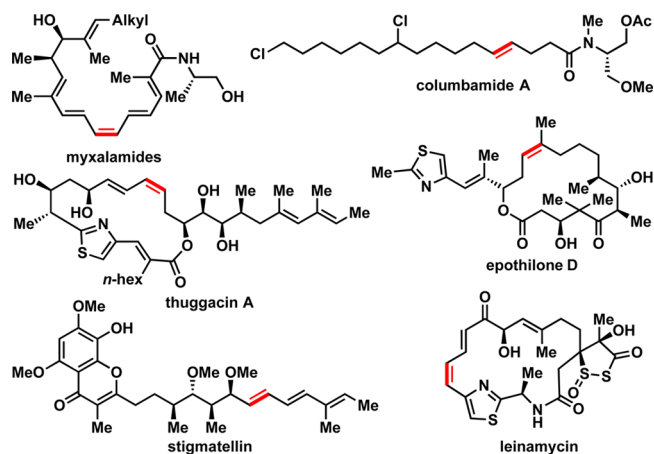


Figure 9. Select examples of sequential dehydration with a missing dehydratase domain. Alkenes arising from modules lacking a DH are highlighted in red. The subsequent module contains an active DH, possibly capable of vinylogous dehydration.

and CurI, while an extraneous DH domain is present in CurF. To uncover the anomalous biosynthetic features of DH catalysis in this segment of the polyketide, we employed diffusible small-molecule truncated NAC thioester substrates in conjunction with LC-MS/MS analysis, site-directed mutagenesis, and co-crystallization studies.

We initially focused on the dehydration event in CurK using a tetraketide substrate and showed that CurK processed it

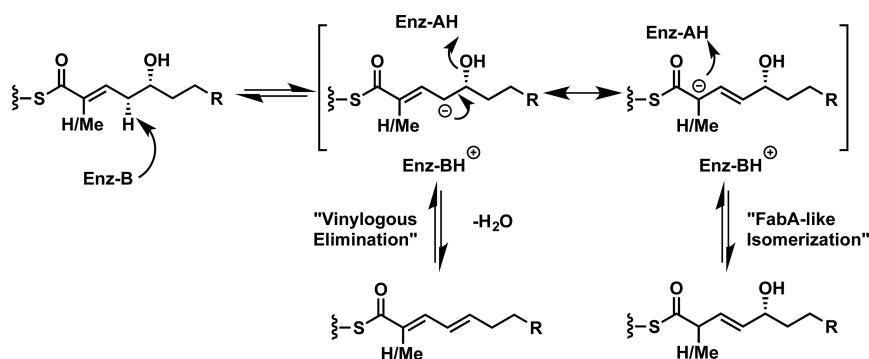


Figure 10. FabA isomerization mechanism and proposed mechanism of vinylogous dehydration by curacin J and H dehydratases. The two events share a common intermediary vinylogous enolate and differ only in the final re-protonation or elimination. Site-directed mutagenesis of the catalytic dyad indicates that the canonical histidine and aspartic residues are the general base and acid, respectively. FabA (*Escherichia coli* β -hydroxydecanoyl thiol ester dehydrase) catalyzes elimination and bond isomerization in fatty acid biosynthesis.

predicted D-alcohol substrate **1** to the *all-trans*-trienoate **7** more than 3 orders of magnitude greater than any previously reported DH with its native substrate,^{27,28} highlighting the high intrinsic activity of Cur DHs when presented with their native substrates. Therefore, the inability of the CurJ-DH, which is the DH domain in the preceding module, to turn over any of the four diastereomeric triketide substrates, including **21**, with the bioinformatically predicted 2*R*,3*S* stereochemistry, suggested an alternative substrate. We hypothesized that CurJ may be responsible for a double dehydration of a β,δ -dihydroxy thioester substrate since the antecedent DH domain is absent in CurI. This would require a canonical dehydration to form a δ -hydroxy- α,β -unsaturated thioester intermediate, which would then undergo a second vinylogous elimination, at the same active site, to afford the *trans,trans*-dienoate product. Using a synthetic triketide δ -hydroxy- α,β -unsaturated thioester substrate, we unequivocally demonstrated that CurJ can catalyze this novel vinylogous elimination as well as the reverse hydration reaction in a completely stereospecific and regio-specific manner. The vinylogous elimination required the His-Asp catalytic dyad as point mutations to either of these residues completely abolished activity. CurH analogously lacks a DH domain in the preceding module and was also shown to catalyze a vinylogous elimination. By contrast, CurK does not catalyze the vinylogous elimination but only the canonical dehydration, as expected on the basis of the collinear organization of CurJ and CurK, which both contain functional DH domains. Interestingly, the substrate specificity of CurF-DH mirrored that of CurK-DH, suggesting CurF-DH is vestigial and may have evolutionarily arisen from an earlier gene duplication event.

To provide a structural framework for the novel vinylogous elimination, we co-crystallized a mutagenized CurJ(H978A) with δ -hydroxy- α,β -unsaturated thioester **21**. The binding pose shows that the catalytic Asp1156 side chain is positioned to hydrogen bond with a hydroxyl group—or water molecule, as in the free-enzyme structures—and that this could be either a β -hydroxy or a δ -hydroxy.

The vinylogous elimination mechanism, catalyzed by both CurH-DH and CurJ-DH, compensates for the two modules lacking dehydratases (CurG and CurI) offering an alternative to the stuttered module hypothesis. The proposed mechanism closely resembles that of FabA in *E. coli*, which catalyzes α,β - to γ,δ -isomerization of unsaturated fatty acids utilizing a His-Asp catalytic dyad. This discovery expands the growing number of

known transformations carried out by the hotdog-fold family of enzymes. More broadly this new mechanism may be operative in other PKS systems missing DH domains.

EXPERIMENTAL SECTION

General Chemistry Procedures. All chemical reagents were used as provided unless indicated otherwise. Freshly distilled reagents were purified as reported.⁴⁶ Tetrahydrofuran (THF) and dichloromethane (CH_2Cl_2) were purified via passage through neutral alumina columns. All reactions were performed under an argon atmosphere using oven-dried (150 °C) glassware. Compounds were purified by flash chromatography using silica gel (300–400 mesh) in the indicated solvent system. Thin-layer chromatography was performed using 250 μm , F254 silica gel plates and visualized by UV or through staining with *p*-anisaldehyde. Optical rotations were acquired on a polarimeter at the indicated temperature using the sodium D line ($\lambda = 589 \text{ nm}$) unless otherwise specified and reported as follows: $[\alpha]_D^{\text{temp}}$ = rotation (c g/100 mL, solvent). ^1H and ^{13}C NMR spectra were recorded on a 400 MHz NMR spectrometer. Chemical shifts are reported in ppm based on an internal standard of residual CHCl_3 (7.26 ppm in ^1H NMR and 77.16 in ^{13}C NMR). Proton chemical data are reported in the following format: chemical shift (ppm), multiplicity (s = singlet, d = doublet, t = triplet, q = quartet, quint = quintet, sext = sextet, sept = septet, m = multiplet, br = broad peak), coupling constant(s), and integration. High-resolution mass spectra (HRMS) were obtained on a time-of-flight (TOF) mass spectrometer using either polyethylene glycol (PEG) or polypropylene glycol (PPG) standards to calibrate the instrument.

Ethyl (2*E*,4*E*)-2-Methylhepta-2,4-dienoate (11). To a solution of triethyl 2-phosphonopropionate (2.81 mL, 13.1 mmol, 1.10 equiv) in THF (36 mL) at 0 °C was added sodium hydride (60% in oil, 0.595 g, 14.9 mmol, 1.25 equiv), and the reaction was stirred for 2 h. Freshly distilled 2-pentenaldehyde **9**⁴⁵ (1.16 mL, 11.9 mmol, 1.00 equiv) was then added dropwise over 20 min. After being stirred at 0 °C for 5.5 h, the reaction was quenched with H_2O (20 mL). The biphasic solution was separated, and the aqueous layer was extracted with Et_2O ($4 \times 20 \text{ mL}$). The combined organic layers were dried (Na_2SO_4), filtered, and concentrated under reduced pressure. Purification by silica gel flash chromatography (95:5 pentane– Et_2O) afforded the title compound (2.00 g, quant.) as a transparent light yellow oil: $R_f = 0.22$ (98:2 pentane– Et_2O); ^1H NMR (CDCl_3 , 400 MHz) δ 7.16 (d, $J = 11.2 \text{ Hz}$, 1H), 6.33 (dd, $J = 14.8, 11.2 \text{ Hz}$, 1H), 6.11 (dt, $J = 15.2, 6.4 \text{ Hz}$, 1H), 4.20 (q, $J = 7.2 \text{ Hz}$, 2H), 2.21 (quint, $J = 7.2 \text{ Hz}$, 2H), 1.93 (s, 3H), 1.30 (t, $J = 7.2 \text{ Hz}$, 3H), 1.05 (t, $J = 7.6 \text{ Hz}$, 3H); ^{13}C NMR (CDCl_3 , 100 MHz) δ 168.8, 144.6, 138.7, 125.3, 125.2, 60.6, 26.5, 14.5, 13.3, 12.7; HRMS (ESI+) m/z calcd for $\text{C}_{10}\text{H}_{16}\text{O}_2\text{Na}^+$ [$M + \text{Na}$] $^+$ 191.1043, found 191.1039 (error 2.1 ppm).

(2*E*,4*E*)-2-Methylhepta-2,4-dienal (13). To a solution of **11** (486 mg, 2.89 mmol, 1.00 equiv) in CH_2Cl_2 (13.0 mL) at 0 °C was slowly added DIBAL-H (1.0 M in hexanes, 6.93 mL, 6.93 mmol, 2.40 equiv).

After 40 min, the reaction was quenched via successive addition of MeOH (3.5 mL) and saturated aqueous sodium potassium tartrate (10.0 mL). The resulting biphasic mixture was stirred vigorously at 23 °C for 14 h. The reaction mixture was partitioned between H₂O (10.0 mL) and CH₂Cl₂ (10 mL). The biphasic mixture was separated, and the aqueous layer was extracted with CH₂Cl₂ (3 × 12 mL). The combined organic layers were dried (Na₂SO₄), filtered, and concentrated under reduced pressure to afford the allylic alcohol **12**, which was carried onto the next reaction without further purification: $R_f = 0.58$ (8:2 hexanes–EtOAc).

To a solution of the crude alcohol **12** prepared above in CH₂Cl₂ (15.0 mL) were sequentially added anhydrous MgSO₄ (1.04 g, 8.67 mmol, 3.00 equiv) and MnO₂ (88% activated, 1.76 g, 20.2 mmol, 7.00 equiv). The resulting gray solution was vigorously stirred at 23 °C for 24 h. The reaction mixture was filtered through a pad of Celite (2.00 cm) and the filtrate concentrated under reduced pressure. Purification by silica gel flash chromatography (98:2 pentane–Et₂O) afforded the title compound (0.345 g, 96% over 2 steps) as a colorless oil: $R_f = 0.43$ (9:1 pentane–Et₂O); ¹H NMR (CDCl₃, 400 MHz) δ 9.42 (s, 1H), 6.83 (d, $J = 11.2$ Hz, 1H), 6.52 (ddt, $J = 14.8, 11.2, 1.6$ Hz, 1H), 6.28 (dt, $J = 14.8, 6.4$ Hz, 1H), 2.32–2.23 (m, 2H), 1.84 (t, $J = 0.8$ Hz, 3H), 1.10 (t, $J = 7.6$ Hz, 3H); ¹³C NMR (CDCl₃, 100 MHz) δ 195.3, 149.5, 147.3, 136.2, 125.1, 26.7, 13.1, 9.5; HRMS (ESI+) m/z calcd for C₈H₁₂ONa⁺ [M + Na]⁺ 147.0780, found 147.0794 (error 9.5 ppm).

(4*R*)-3-[(3*S*,4*E*,6*E*)-3-Hydroxy-4-methylnona-4,6-dienoyl]-4-isopropylthiazolidine-2-thione (**15**). To a solution of **14** (0.484 g, 2.38 mmol, 1.60 equiv) in CH₂Cl₂ (12.0 mL) at –40 °C was added TiCl₄ (0.277 mL, 2.53 mmol, 1.70 equiv), whereupon the solution changed from bright yellow to orange-red. The solution was stirred for 30 min at –40 °C, and then freshly distilled iPr₂NEt (0.441 mL, 2.53 mmol, 1.70 equiv) was added dropwise. After 2.25 h, the blood-red solution was cooled to –78 °C, and aldehyde **13** (185.0 mg, 1.49 mmol, 1.00 equiv, dried overnight over 3 Å molecular sieves) was added over 1 min. The aldol reaction was stirred at –78 °C for 3.5 h and quenched with saturated aqueous NH₄Cl (6.0 mL). The biphasic solution was separated, and the aqueous layer was extracted with CH₂Cl₂ (4 × 10 mL). The combined organics were dried (Na₂SO₄), filtered, and concentrated under reduced pressure. Purification by silica gel flash chromatography (7:3 hexane–EtOAc) afforded the title compound (0.230 g, 47%) as a viscous bright yellow oil: $R_f = 0.41$ (7:3 hexane–EtOAc); $[\alpha]_D^{24} = -246$ (c 1.00, CHCl₃); ¹H NMR (CDCl₃, 400 MHz) δ 6.24 (dd, $J = 14.8, 10.8$ Hz, 1H), 6.09 (d, $J = 10.8$ Hz, 1H), 5.76 (dt, $J = 14.8, 6.8$ Hz, 1H), 5.14 (t, $J = 6.8$ Hz, 1H), 4.61 (dd, $J = 8.8, 0.8$ Hz, 1H), 3.59–3.48 (m, 2H), 3.42 (dd, $J = 17.2, 9.2$ Hz, 1H), 3.03 (d, $J = 11.6$ Hz, 1H), 2.65 (br s, 1H), 2.37 (sext, $J = 6.4$ Hz, 1H), 2.13 (pent, $J = 7.2$ Hz, 2H), 1.77 (s, 3H), 1.06 (d, $J = 6.8$ Hz, 3H), 1.02 (d, $J = 7.4$ Hz, 3H), 0.99 (t, $J = 8.8$ Hz, 3H); ¹³C NMR (CDCl₃, 100 MHz) δ 203.2, 172.9, 137.5, 135.2, 125.9, 124.9, 73.0, 71.7, 44.1, 31.0, 30.8, 26.2, 19.2, 18.0, 13.8, 13.0; HRMS (ESI+) m/z calcd for C₁₆H₂₃NO₂S₂Na⁺ [M + Na]⁺ 350.1219, found 350.1207 (error 3.4 ppm).

5-(2-Acetamidoethyl) (4*S*,6*E*)-3-Hydroxy-4-methylnona-4,6-dienethioate (**1**). A solution of aldol adduct **15** (15.0 mg, 0.0458 mmol, 1.00 equiv) in CH₂Cl₂ (3.00 mL) was treated with NAC (5.0 μ L, 0.050 mmol, 1.1 equiv) and imidazole (9.4 mg, 0.14 mmol, 3.0 equiv) and stirred at 23 °C for 22 h. The reaction mixture was partitioned between H₂O (5 mL) and EtOAc (5 mL), and the layers were separated. The aqueous layer was extracted with EtOAc (4 × 10 mL), and the combined organic fractions were dried (Na₂SO₄), filtered, and concentrated under reduced pressure. The crude residue was purified by flash chromatography (95:5 CH₂Cl₂–MeOH) to afford the title compound (7.2 mg, 55%) as a colorless oil: $R_f = 0.39$ (95:5 CH₂Cl₂–MeOH); $[\alpha]_D^{24} = -21$ (c 0.52, CHCl₃); ¹H NMR (CDCl₃, 400 MHz) δ 6.22 (dd, $J = 15.2, 10.4$ Hz, 1H), 6.07 (d, $J = 10.8$ Hz, 1H), 5.83 (br s, 1H), 5.76 (dt, $J = 15.2, 6.4$ Hz, 1H), 4.53 (dd, $J = 9.2, 3.6$ Hz, 1H), 3.48–3.40 (m, 2H), 3.05 (app. sext, $J = 8.0$ Hz, 2H), 2.84 (dd, $J = 15.2, 8.8$ Hz, 1H), 2.76 (dd, $J = 14.8, 4.0$ Hz, 1H), 2.48 (br s, 1H), 2.13 (app. quint, $J = 7.2$ Hz, 2H), 1.96 (s, 3H), 1.75 (s, 3H), 1.01 (t, $J = 7.2$ Hz, 3H); ¹³C NMR (CDCl₃, 100 MHz) δ 199.0, 170.6, 138.0, 134.9, 126.3, 124.7, 74.0, 49.6, 39.5, 29.0, 26.1,

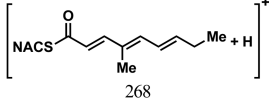
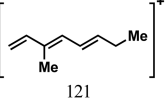
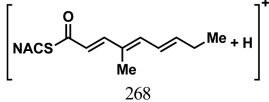
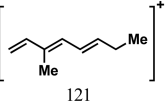
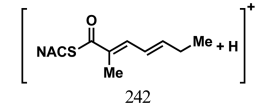
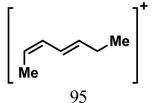
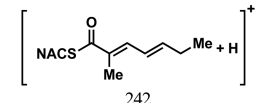
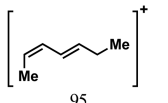
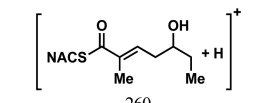
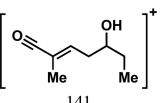
23.4, 13.8, 12.6; HRMS (ESI+) m/z calcd for C₁₄H₂₃NO₃SN⁺ [M + Na]⁺ 308.1291, found 308.1275 (error 5.2 ppm).

(4*R*)-4-Benzyl-3-[(2*S*,3*R*,4*E*)-3-hydroxy-2-methylhept-4-enoyl]-thiazolidine-2-thione (**18**). To a solution of thiazolidinethione **17** (0.250 g, 0.940 mmol, 1.00 equiv) in CH₂Cl₂ (4.00 mL) at 0 °C was added TiCl₄ (0.110 mL, 0.990 mmol, 1.05 equiv). The resulting bright orange, opaque solution was stirred for 9 min. Next, freshly distilled iPr₂EtN (0.183 mL, 1.05 mmol, 1.12 equiv) was added, and the reaction was further stirred for 40 min at 0 °C. To the dark red mixture was slowly added freshly distilled 2-pentenaldehyde (0.138 mL, 1.41 mmol, 1.50 equiv), causing a color change to dark brown. After 2 h, the reaction was quenched with saturated aqueous NH₄Cl (5 mL). The biphasic mixture was warmed to 23 °C, and the layers were separated. The aqueous layer was extracted with CH₂Cl₂ (3 × 10 mL), and the combined organic layers were dried (Na₂SO₄), filtered, and concentrated under reduced pressure. Purification by flash chromatography (8:2 hexanes–EtOAc) afforded the title compound (0.252 g, 72%) as a viscous, yellow oil: $R_f = 0.20$ (8:2 hexanes–EtOAc); $[\alpha]_D^{22} = -191.6$ (c 1.00, CHCl₃); ¹H NMR (CDCl₃, 400 MHz) δ 7.37–7.27 (m, 5H), 5.82 (ddt, $J = 15.6, 6.4, 1.2$ Hz, 1H), 5.50 (ddt, $J = 15.2, 6.0, 1.2$ Hz, 1H), 5.39 (ddd, $J = 10.6, 6.8, 4$ Hz, 1H), 4.79 (dq, $J = 6.8, 3.2$ Hz, 1H), 4.59–4.54 (m, 1H), 3.37 (dd, $J = 11.6, 6.8$ Hz, 1H), 3.24 (dd, $J = 13.2, 4.0$ Hz, 1H), 3.04 (dd, $J = 13.2, 10.4$ Hz, 1H), 2.88 (d, $J = 11.6$ Hz, 1H), 2.74 (d, $J = 2.8$ Hz, 1H), 2.08 (app. quint, $J = 7.2, 2$ Hz), 1.19 (d, $J = 6.8$ Hz, 3H), 1.01 (t, $J = 7.6$ Hz, 3H); ¹³C NMR (CDCl₃, 100 MHz) δ 201.8, 177.8, 136.6, 135.0, 129.6, 129.1, 127.9, 127.4, 72.5, 69.1, 43.5, 37.1, 31.9, 25.5, 13.6, 11.6; HRMS (ESI+) m/z calcd for C₁₈H₂₃NO₂S₂Na⁺ [M + Na]⁺ 372.1062, found 372.1087 (error 6.7 ppm).

(4*R*)-4-Benzyl-3-[(2*R*,3*R*,4*E*)-3-hydroxy-2-methylhept-4-enoyl]-thiazolidine-2-thione (**19**). To a solution of **17** (0.150 g, 0.566 mmol, 1.00 equiv) in anhydrous EtOAc (1.4 mL) were sequentially added anhydrous MgBr₂·OEt₂ (14.6 mg, 0.0566 mmol, 0.100 equiv), 2-pentenaldehyde (60.9 μ L, 0.623 mmol, 1.10 equiv), Et₃N (0.158 mmol, 1.13 mmol, 2.00 equiv), and Me₃SiCl (0.108 mL, 0.849 mmol, 1.50 equiv), which all had been freshly distilled. The reaction mixture was stirred at 23 °C for 26 h and then filtered through a silica gel plug (2.00 cm), washing with Et₂O (20 mL), and the filtrate was concentrated under reduced pressure. The crude residue was dissolved in a biphasic mixture of THF (10 mL) and aqueous hydrochloric acid (1 N, 2 mL) and vigorously stirred at 23 °C for 2 h. The reaction was then quenched with saturated aqueous sodium bicarbonate (10 mL), and the biphasic solution was separated. The aqueous layer was extracted with EtOAc (3 × 15 mL), and the combined organic fractions were dried (Na₂SO₄), filtered, and concentrated under reduced pressure. Purification by silica gel flash chromatography (8:2 hexane–EtOAc) afforded the title compound (35.8 mg, 17%) as a viscous, yellow oil: $R_f = 0.28$ (8:2 hexane–EtOAc); $[\alpha]_D^{24} = -297.1$ (c 1.00, CHCl₃); ¹H NMR (CDCl₃, 400 MHz) δ 7.37–7.27 (m, 5H), 5.79 (dt, $J = 15.2, 5.6$ Hz, 1H), 5.42 (ddt, $J = 15.2, 7.2, 1.6$ Hz, 1H), 5.25 (ddd, $J = 10.8, 6.8, 3.6$ Hz, 1H), 4.34 (dq, $J = 7.6, 6.8$ Hz, 1H), 4.26 (t, $J = 7.6$ Hz, 1H), 3.39 (dd, $J = 11.2, 6.8$ Hz, 1H), 3.26 (dd, $J = 13.2, 3.6$ Hz, 1H), 3.06 (dd, $J = 12.8, 10.8$ Hz, 1H), 2.90 (d, $J = 11.6$ Hz, 1H), 2.16 (br, 1H), 2.06 (app. quint, $J = 6.4, 2$ Hz), 1.22 (d, $J = 6.8$ Hz, 3H), 1.00 (t, $J = 7.2$ Hz, 3H); ¹³C NMR (CDCl₃, 100 MHz) δ 201.5, 178.2, 136.7, 136.3, 129.6, 129.3, 129.0, 127.3, 76.7, 69.2, 45.2, 36.8, 32.8, 25.4, 14.9, 13.5; HRMS (ESI+) m/z calcd for C₁₈H₂₃NO₂S₂Na⁺ [M + Na]⁺ 372.1062, found 372.1049 (error 3.5 ppm).

5-(2-Acetamidoethyl) (2*R*,3*R*,4*E*)-3-Hydroxy-2-methylhept-4-ene-thioate (**3**). To a solution of **19** (31.1 mg, 0.0890 mmol, 1.00 equiv) in CH₂Cl₂ (4.00 mL) were added imidazole (18.2 mg, 0.267 mmol, 3.00 equiv) and NAC (10.4 μ L, 0.0980 mmol, 1.10 equiv). The reaction mixture was vigorously stirred at 23 °C for 21 h. The crude reaction mixture was concentrated under reduced pressure and directly purified by flash chromatography (95:5 CH₂Cl₂–MeOH) to afford the title compound (16.8 mg, 67%) as a light yellow, viscous oil: $R_f = 0.30$ (95:5 CH₂Cl₂–MeOH); $[\alpha]_D^{24} = -34.5$ (c 0.29, CHCl₃); ¹H NMR (CDCl₃, 400 MHz) δ 6.00 (br s, 1H), 5.76 (dt, $J = 15.6, 6.0$ Hz, 1H), 5.40 (ddt, $J = 15.6, 6.4, 1.2$ Hz, 1H), 4.19 (t, $J = 7.6$ Hz, 1H), 3.55–

Table 2. LC-MS/MS Transitions, Parameters, and Retention Times for 1–8, 20, and 21

Cmpd	Precursor Ion (<i>m/z</i>)	Product Ion (<i>m/z</i>)	DP ^a (V)	CE ^a (V)	CXP ^a (V)	Retention Time (min)
1, 2	 268	 121	35	25	15	6.17
7	 268	 121	35	25	15	7.44
3, 4, 5, 6	 242	 95	35	30	15	5.52 (3 and 6) 5.24 (4 and 5)
8	 242	 95	35	30	15	6.80
20, 21	 260	 141	35	17	15	5.11

^aMass spectrometry parameter abbreviations: DP, de-clustering potential; CE, collision energy; CXP, collision cell exit potential.

3.37 (m, 2H), 3.13–2.98 (m, 2H), 2.76 (app. quint, *J* = 7.2 Hz, 1H), 2.42 (br s, 1H), 2.06 (app. quint, *J* = 7.6 Hz, 2H), 1.94 (s, 3H), 1.11 (d, *J* = 6.8 Hz, 3H), 1.00 (t, *J* = 7.6 Hz, 3H); ¹³C NMR (CDCl₃, 100 MHz) δ 203.6, 170.6, 136.6, 128.8, 75.5, 54.5, 39.5, 28.7, 25.4, 23.3, 15.1, 13.5; HRMS (ESI+) *m/z* calcd for C₁₂H₂₁NO₃SNa⁺ [*M* + Na]⁺ 282.1134, found 282.1153 (error 6.7 ppm).

General Biology Procedures. All chemical reagents were purchased from Sigma-Aldrich and were used directly without further purification. *E. coli* BL21(DE3) cells were from New England BioLabs. Isopropyl β-D-1-thiogalactopyranoside (IPTG) was acquired through Gold Biotechnology. His60 Ni Superflow resin was purchased from Clontech Laboratories, Inc. OD₆₀₀ was measured on an Eppendorf BioPhotometer. Sonication was carried out with a Branson Sonifier 450. Gel filtration purification was performed on HiLoad 16/600 Superdex 200 pg column (GE Healthcare). The protein mass spectra data were obtained on a Bruker BioTOF II mass spectrometer. LC-MS/MS was conducted with an AB Sciex QTRAP 5500 mass spectrometer and Shimadzu LC system.

Protein Purification and Crystallization. DHs were purified as described previously.¹⁰ For co-crystallization of substrates with inactive CurJ-DH variants, the protein was pre-incubated 2 h on ice in 5 mM substrate and then crystallized at 20 °C by sitting-drop vapor diffusion from a 1:1 mixture of protein stock (15 mg/mL DH, 5 mM substrate, 50 mM Tris pH 7.5, 150 mM NaCl, 10% glycerol) with well solution (18% PEG 3350, 5% 1,4-butanediol, 250 mM NaCl, 100 mM Bis-Tris propane pH 6.5). Crystals were harvested directly from drops into liquid N₂.

Data Collection and Structure Determination. Data were collected at the Advanced Photon Source (APS, Argonne National Laboratory) on GM/CA beamline 23ID-D. CurJ H978F crystals diffracted to 2.4 Å in the presence of 5 mM substrate. The crystals were nearly isomorphous with the previously reported crystals of wild-type CurJ-DH.¹⁰ Data were processed using XDS.⁴⁷ The structure was solved by molecular replacement in PHENIX⁴⁸ using the wild-type CurJ (PDB 3KG8) as a search model. Refinement was accomplished in PHENIX and model building with coot.⁴⁹ Ligand restraint files were built using eLBOW⁵⁰ in PHENIX. The structure was validated with MolProbity;⁵¹ figures were generated with PyMOL.⁵²

Steady-State Kinetic Studies of CurK-DH. Incubation and Sample Preparation. Substrate 1 (0.25–6.0 mM) was incubated with recombinant CurK-DH (20 nM) and reaction buffer (50 mM Tris, 150 mM NaCl, pH 8.0) in a total volume of 50 μL at 23 °C. The

reaction was quenched at 4 min by transfer of 5 μL of the reaction mixture into 495 μL of quench solution (1:1 MeCN–H₂O). The quenched mixture was briefly vortexed and centrifuged (21000g, 5 min). A portion of the centrifuged supernatant (60 μL) was transferred to an HPLC vial containing the internal standard (10 μL of a 320 nM solution of diene 8), mixed, injected, and analyzed by LC-MS/MS.

Instrumentation. Reverse-phase liquid chromatography was conducted on a Shimadzu UFLC XR chromatograph, SIL-20AC autosampler, and Prominence CTO-20A column oven. A SCIEX QTRAP 5500 instrument (Framingham, MA) was used for mass detection with an electrospray ionization source. All instrumentation was run using Analyst software (1.5.2, AB SCIEX).

Chromatography. Reverse phase HPLC was conducted using a Kinetix reverse-phase C₁₈ column (50 mm × 2.1 mm, 2.6 μm, Phenomenex, Torrance, CA) operated at 0.4 mL min⁻¹ with a column temperature of 35 °C. The mobile phase A (0.1% formic acid in H₂O) and mobile phase B (acetonitrile) were run at the following gradient program: 0 min, 5% B; 2 min, 5% B; 7 min, 55% B; 8 min, 70% B; 9 min, 70% B; 10.5 min, 5% B; 12 min, 5% B, STOP. The injection volume was 10 μL.

Mass Spectrometry. Analytes were analyzed by MS in positive ionization mode by Multiple Reaction Monitoring (MRM). Optimal MRM settings were determined by direct infusion of the analyte solution (10 nM, 1:1 H₂O–MeCN with 0.1% formic acid) onto the MS by a syringe pump at a flow of 10 μL/min. The transitions and retention times are displayed in Table 2.

Standard Curve and Data Analysis. A standard curve for the triene product 7 was generated by injecting the authentic standard at varying concentrations with a fixed concentration of internal standard 8. Transitions and retention times are given in Table S1. Analyte and internal standard peak areas were calculated using MultiQuant software (version 2.0.2). Each analyte peak area was normalized to internal standard (8) peak area and converted to an analyte concentration using the standard curve equation. Each reaction was performed in duplicate. The calculated initial velocity at each substrate concentration was used to generate a Michaelis–Menten curve (eq 1,

$$v = \frac{V_{\max}[S]}{K_M + [S]} \quad (1)$$

Figure S3) utilizing Prism 5 software (Version 5.0b) (Figure S2), where v is the reaction rate, V_{\max} is the maximum enzymatic reaction rate, $[S]$ is the concentration of substrate, and K_M is the Michaelis–Menten constant.

Overnight Incubation of Cur DHs with Synthetic NAC Substrates. Incubations were carried out following a similar procedure to that of the kinetic analysis of CurK-DH. Briefly, substrates **1–6**, **20**, and **21**, and product **8** (1 mM), were individually incubated with enzyme (5 μ M) (CurF-DH, CurH-DH, CurJ-DH, and CurK-DH) in reaction buffer (50 mM Tris, 150 mM NaCl, pH 8.0) at 23 °C for 14 h (or a set time period in the case of the CurK-DH time course experiment) in a total volume of 100 μ L. Samples (5 μ L) were quenched with 495 μ L quench solution (1:1 MeCN–H₂O). The mixture was centrifuged, and the supernatant was directly analyzed by LC-MS/MS using the method described above. Chromatograms were generated by extraction of raw the LC-MS/MS data with Analyst software and plotted with Prism software.

Chemoenzymatic Synthesis of **1 by CurK-DH: 5-(2-Acetamidoethyl) (2E,4E,6E)-4-Methylnona-2,4,6-trienethioate (**7**).** A solution of sterile H₂O (3.82 mL) and a small amount of 10X TRIS buffer solution (1.50 M NaCl, 0.500 M TRIS-HCl, pH 8.0) (0.600 mL) was briefly vortexed. To the buffered solution was added a DMSO–H₂O (1:1) stock solution (50 mM) of the β -hydroxy thioester substrate **1** (0.700 mL, 10.0 mg, 35.0 μ mol). The mixture was vortexed to mix, and the CurK-DH (8.19 mg/mL, 0.684 mL, 5.60 mg, 0.160 μ mol) was added. The mixture was briefly inverted and covered with aluminum foil to shield from light. The reaction mixture was shaken (200 rpm) at 23 °C in the dark for 14 h. The reaction mixture was extracted with EtOAc (4 \times 10.0 mL), and the combined extracts were dried (Na₂SO₄), filtered, and concentrated under reduced pressure. The crude extract was purified by flash chromatography (95:5 CH₂Cl₂–MeOH) affording the title compound (2.52 mg, 25%) as a transparent light yellow oil: R_f = 0.35 (95:5 CH₂Cl₂–MeOH); ¹H NMR (CDCl₃, 400 MHz) δ 7.30 (d, J = 15.6 Hz, 1H), 6.46 (d, J = 11.2 Hz, 1H), 6.40 (app. t, J = 13.6 Hz, 1H), 6.15 (d, J = 15.2 Hz, 1H), 6.05 (dt, J = 13.6, 6.4 Hz, 1H), 5.98 (br, 1H), 3.48 (q, J = 6.0 Hz, 2H), 3.12 (t, J = 6.4 Hz, 2H), 2.22 (app. quint, J = 6.8 Hz, 2H), 1.97 (s, 3H), 1.87 (s, 3H), 1.06 (t, J = 7.6 Hz, 3H); ¹³C NMR (CDCl₃, 100 MHz) δ 190.5, 170.6, 146.5, 143.6, 141.6, 131.2, 125.8, 122.8, 40.3, 28.5, 26.6, 23.4, 13.4, 12.5; HRMS (ESI+) m/z calcd for C₁₄H₂₁NO₂SNa⁺ [M + Na]⁺ 290.1185, found 290.1208 (error 7.9 ppm).

■ ASSOCIATED CONTENT

● Supporting Information

The Supporting Information is available free of charge on the ACS Publications website at DOI: 10.1021/jacs.6b09748.

Full ¹H and ¹³C NMR spectra of all described compounds, procedures for the synthesis of compounds **8**, **20**, and **21**, as well as LC–MS/MS data, included as Figures S1 and S2 and Tables S1 and S2; Figure S3 depicts ligand omit difference density; the Curacin DH structures have been deposited in the PDB as entries 5TZ5, 5TZ6, and 5TZ7 (PDF)

■ AUTHOR INFORMATION

Corresponding Author

*aldri015@umn.edu

ORCID

Courtney C. Aldrich: 0000-0001-9261-594X

Notes

The authors declare no competing financial interest.

■ ACKNOWLEDGMENTS

This work was supported by a grant (GM081544 to J.L.S.) from the National Institutes of Health. Mass spectrometry was

carried out with the assistance of Dr. Bruce A. Witthuhn in the Analytical Biochemistry Shared Resource of the Masonic Cancer Center, University of Minnesota, funded in part by Cancer Center Support Grant CA-77598. We also gratefully acknowledge financial support from the Department of Medicinal Chemistry, University of Minnesota (to W.D.F.).

■ REFERENCES

- (1) Gerwick, W. H.; Proteau, P. J.; Nagle, D. G.; Hamel, E.; Blokhin, A.; Slate, D. L. *J. Org. Chem.* **1994**, *59*, 1243.
- (2) Gu, L.; Wang, B.; Kulkarni, A.; Geders, T. W.; Grindberg, R. V.; Gerwick, L.; Hakansson, K.; Wipf, P.; Smith, J. L.; Gerwick, W. H.; Sherman, D. H. *Nature* **2009**, *459*, 731.
- (3) Gu, L.; Wang, B.; Kulkarni, A.; Gehret, J. J.; Lloyd, K. R.; Gerwick, L.; Gerwick, W. H.; Wipf, P.; Håkansson, K.; Smith, J. L.; Sherman, D. H. *J. Am. Chem. Soc.* **2009**, *131*, 16033.
- (4) Gu, L.; Eisman, E. B.; Dutta, S.; Franzmann, T. M.; Walter, S.; Gerwick, W. H.; Skiniotis, G.; Sherman, D. H. *Angew. Chem., Int. Ed.* **2011**, *50*, 2795.
- (5) McCarthy, J. G.; Eisman, E. B.; Kulkarni, S.; Gerwick, L.; Gerwick, W. H.; Wipf, P.; Sherman, D. H.; Smith, J. L. *ACS Chem. Biol.* **2012**, *7*, 1994.
- (6) Khare, D.; Wang, B.; Gu, L.; Razelun, J.; Sherman, D. H.; Gerwick, W. H.; Håkansson, K.; Smith, J. L. *Proc. Natl. Acad. Sci. U. S. A.* **2010**, *107*, 14099.
- (7) Khare, D.; Hale, W. A.; Tripathi, A.; Gu, L.; Sherman, D. H.; Gerwick, W. H.; Håkansson, K.; Smith, J. L. *Structure* **2015**, *23*, 2213.
- (8) Gu, L.; Geders, T. W.; Wang, B.; Gerwick, W. H.; Håkansson, K.; Smith, J. L.; Sherman, D. H. *Science* **2007**, *318*, 970.
- (9) Whicher, J. R.; Smaga, S. S.; Hansen, D. A.; Brown, W. C.; Gerwick, W. H.; Sherman, D. H.; Smith, J. L. *Chem. Biol.* **2013**, *20*, 1340.
- (10) Akey, D. L.; Razelun, J. R.; Tehranisa, J.; Sherman, D. H.; Gerwick, W. H.; Smith, J. L. *Structure* **2010**, *18*, 94.
- (11) Gehret, J. J.; Gu, L.; Gerwick, W. H.; Wipf, P.; Sherman, D. H.; Smith, J. L. *J. Biol. Chem.* **2011**, *286*, 14445.
- (12) Geders, T. W.; Gu, L.; Mowers, J. C.; Liu, H.; Gerwick, W. H.; Håkansson, K.; Sherman, D. H.; Smith, J. L. *J. Biol. Chem.* **2007**, *282*, 35954.
- (13) Akey, D. L.; Gehret, J. J.; Khare, D.; Smith, J. L. *Nat. Prod. Rep.* **2012**, *29*, 1038.
- (14) Yoo, H.-D.; Gerwick, W. H. *J. Nat. Prod.* **1995**, *58*, 1961.
- (15) Chang, Z.; Sitachitta, N.; Rossi, J. V.; Roberts, M. A.; Flatt, P. M.; Jia, J.; Sherman, D. H.; Gerwick, W. H. *J. Nat. Prod.* **2004**, *67*, 1356.
- (16) Moss, S. J.; Martin, C. J.; Wilkinson, B. *Nat. Prod. Rep.* **2004**, *21*, 575.
- (17) Helmkamp, G. M.; Bloch, K. *J. Biol. Chem.* **1969**, *244*, 6014.
- (18) Leesong, M.; Henderson, B. S.; Gillig, J. R.; Schwab, J. M.; Smith, J. L. *Structure* **1996**, *4*, 253.
- (19) Nagao, Y.; Hagiwara, Y.; Kumagai, T.; Ochiai, M.; Inoue, T.; Hashimoto, K.; Fujita, E. *J. Org. Chem.* **1986**, *51*, 2391.
- (20) Crimmins, M. T.; Chaudhary, K. *Org. Lett.* **2000**, *2*, 775.
- (21) Evans, D. A.; Downey, C. W.; Shaw, J. T.; Tedrow, J. S. *Org. Lett.* **2002**, *4*, 1127.
- (22) Wadsworth, W. S.; Emmons, W. D. *J. Am. Chem. Soc.* **1961**, *83*, 1733.
- (23) Rathke, M. W.; Nowak, M. *J. Org. Chem.* **1985**, *50*, 2624.
- (24) Zheng, J.; Taylor, C. A.; Piasecki, S. K.; Keatinge-Clay, A. T. *Structure* **2010**, *18*, 913.
- (25) Caffrey, P. *ChemBioChem* **2003**, *4*, 654.
- (26) Reid, R.; Piagentini, M.; Rodriguez, E.; Ashley, G.; Viswanathan, N.; Carney, J.; Santi, D. V.; Hutchinson, C. R.; McDaniel, R. *Biochemistry* **2003**, *42*, 72.
- (27) Fiers, W. D.; Dodge, G. J.; Li, Y.; Smith, J. L.; Fecik, R. A.; Aldrich, C. C. *Chem. Sci.* **2015**, *6*, 5027.
- (28) Li, Y.; Dodge, G. J.; Fiers, W. D.; Fecik, R. A.; Smith, J. L.; Aldrich, C. C. *J. Am. Chem. Soc.* **2015**, *137*, 7003.

- (29) Keatinge-Clay, A. T. *Chem. Biol.* **2007**, *14*, 898.
- (30) Tang, L.; Ward, S.; Chung, L.; Carney, J. R.; Li, Y.; Reid, R.; Katz, L. J. *Am. Chem. Soc.* **2004**, *126*, 46.
- (31) Tang, G.-L.; Cheng, Y.-Q.; Shen, B. *Chem. Biol.* **2004**, *11*, 33.
- (32) Buntin, K.; Irschik, H.; Weissman, K. J.; Luxenburger, E.; Blöcker, H.; Müller, R. *Chem. Biol.* **2010**, *17*, 342.
- (33) Gaitatzis, N.; Silakowski, B.; Kunze, B.; Nordsiek, G.; Blöcker, H.; Höfle, G.; Müller, R. *J. Biol. Chem.* **2002**, *277*, 13082.
- (34) Kleigrew, K.; Almaliti, J.; Tian, I. Y.; Kinnel, R. B.; Korobeynikov, A.; Monroe, E. A.; Duggan, B. M.; Di Marzo, V.; Sherman, D. H.; Dorrestein, P. C.; Gerwick, L.; Gerwick, W. H. *J. Nat. Prod.* **2015**, *78*, 1671.
- (35) Dickschat, J. S.; Vergnolle, O.; Hong, H.; Garner, S.; Bidgood, S. R.; Dooley, H. C.; Deng, Z.; Leadlay, P. F.; Sun, Y. *ChemBioChem* **2011**, *12*, 2408.
- (36) Castonguay, R.; Valenzano, C. R.; Chen, A. Y.; Keatinge-Clay, A.; Khosla, C.; Cane, D. E. *J. Am. Chem. Soc.* **2008**, *130*, 11598.
- (37) Sedgwick, B.; Morris, C.; French, S. J. *J. Chem. Soc., Chem. Commun.* **1978**, 193.
- (38) Gay, D. C.; Spear, P. J.; Keatinge-Clay, A. T. *ACS Chem. Biol.* **2014**, *9*, 2374.
- (39) Lohr, F.; Jenniches, I.; Frizler, M.; Meehan, M. J.; Sylvester, M.; Schmitz, A.; Gutschow, M.; Dorrestein, P. C.; König, G. M.; Schaberle, T. F. *Chem. Sci.* **2013**, *4*, 4175.
- (40) Schwab, J. M.; Klassen, J. B. *J. Am. Chem. Soc.* **1984**, *106*, 7217.
- (41) Schupp, T.; Toupet, C.; Engel, N.; Goff, S. *FEMS Microbiol. Lett.* **1998**, *159*, 201.
- (42) Caffrey, P.; Lynch, S.; Flood, E.; Finnan, S.; Oliynyk, M. *Chem. Biol.* **2001**, *8*, 713.
- (43) Motamedi, H.; Shafiee, A. *Eur. J. Biochem.* **1998**, *256*, 528.
- (44) Molnár, I.; Schupp, T.; Ono, M.; Zirkle, R. E.; Milnamow, M.; Nowak-Thompson, B.; Engel, N.; Toupet, C.; Stratmann, A.; Cyr, D. D.; Grolach, J.; Mayo, J. M.; Hu, A.; Goff, S.; Schmid, J.; Ligon, J. M. *Chem. Biol.* **2000**, *7*, 97.
- (45) In curacin biosynthetic nomenclature, proteins and modules are only designated by an equivalent, alphabetical identity. The CurF ER domain is considered part of the hydroxymethyl-glutaryl-CoA synthase cassette for β -branching and is appended onto the first PKS module (module F). To draw an analogy between traditional PKS pathways, this has been simplified to include the ER in the Cur F PKS module.
- (46) Armarego, W. L. F.; Perrin, D. D. *Purification of laboratory chemicals*, 4th ed.; Butterworth Heinemann: Oxford/Boston, 1996.
- (47) Kabsch, W. *Acta Crystallogr., Sect. D: Biol. Crystallogr.* **2010**, *66*, 125–132.
- (48) Adams, P. D.; Afonine, P. V.; Bunkóczi, G.; Chen, V. B.; Davis, I. W.; Echols, N.; Headd, J. J.; Hung, L.-W.; Kapral, G. J.; Grosse-Kunstleve, R. W.; McCoy, A. J.; Moriarty, N. W.; Oeffner, R.; Read, R. J.; Richardson, D. C.; Richardson, J. S.; Terwilliger, T. C.; Zwart, P. H. *Acta Crystallogr., Sect. D: Biol. Crystallogr.* **2010**, *66*, 213–221.
- (49) Emsley, P.; Lohkamp, B.; Scott, W. G.; Cowtan, K. *Acta Crystallogr., Sect. D: Biol. Crystallogr.* **2010**, *66*, 486–501.
- (50) Moriarty, N. W.; Grosse-Kunstleve, R. W.; Adams, P. D. *Acta Crystallogr., Sect. D: Biol. Crystallogr.* **2009**, *65*, 1074–1080.
- (51) Chen, V. B.; Arendall, W. B., III; Headd, J. J.; Keedy, D. A.; Immormino, R. M.; Kapral, G. J.; Murray, L. W.; Richardson, J. S.; Richardson, D. C. *Acta Crystallogr., Sect. D: Biol. Crystallogr.* **2010**, *66*, 12–21.
- (52) *The PyMol Molecular Graphics System*, Version 1.3–1.4, Schrodinger, LLC; <http://www.pymol.org/>.